Journal of Marine Science and Technology

Volume 27 | Issue 3 Article 6

THE EFFECT OF HYDRO-METEOROLOGY ON SHIP COLLISION AVOIDANCE IN HEAVY TRAFFIC AREAS WITH A SIMPLIFIED SIMULATION MODEL

Ming-Chung Fang
Department of Systems and Naval Mechatronic Engineering, National Cheng Kung University , Tainan, Taiwan, R.O.C

Kun-Yuan Tsai
Department of Systems and Naval Mechatronic Engineering, National Cheng Kung University , Tainan, Taiwan, R.O.C

Chih-Chung Fang
Department of Systems Engineering and Naval Architecture, National Taiwan Ocean University, Keelung, Taiwan, R.O.C.

Recommended Citation
Fang, Ming-Chung; Tsai, Kun-Yuan; and Fang, Chih-Chung (2019) "THE EFFECT OF HYDRO-METEOROLOGY ON SHIP COLLISION AVOIDANCE IN HEAVY TRAFFIC AREAS WITH A SIMPLIFIED SIMULATION MODEL," *Journal of Marine Science and Technology*: Vol. 27: Iss. 3, Article 6.
DOI: 10.6119/JMST.201906_27(3).0006
Available at: https://jmstt.ntou.edu.tw/journal/vol27/iss3/6

THE EFFECT OF HYDRO-METEOROLOGY ON SHIP COLLISION AVOIDANCE IN HEAVY TRAFFIC AREAS WITH A SIMPLIFIED SIMULATION MODEL

Acknowledgements

The authors wish to thank the Ministry of Science and Technology, Republic of China (MOST-104-2221-E-006-199-MY3), for its financial support.

Journal of Marine Science and Technology, Vol. 27, No. 3, pp. 235-245 (2019)
DOI: 10.6119/JMST.201906_27(3).0006

THE EFFECT OF HYDRO-METEOROLOGY ON SHIP COLLISION AVOIDANCE IN HEAVY TRAFFIC AREAS WITH A SIMPLIFIED SIMULATION MODEL

Ming-Chung Fang[1], Kun-Yuan Tsai[1], and Chih-Chung Fang[2]

Key words: hydro-meteorology, nomoto's second-order model, multi-ship encounter, sea trial.

ABSTRACT

On the basis of the ship collision avoidance steering system in calm water developed by the authors, this paper upgrades the numerical simulation model by considering various hydro-meteorological factors for ships with nonuniform movement. A real-time simulator was used for the numerical simulation of the container ship. To clarify the validity of the maneuvering mathematical model, sea trial results for the container ship were compared with the results for the present simulation system in terms of turn trajectory. In this study, a numerical technique based on Nomoto's second-order model was employed to investigate the turning characteristics of a container ship. The maneuvering indices were obtained from numerical simulations using the Newton-Raphson method and a regression technique. Both simple and complex collision avoidance cases were selected to verify the proposed ship collision avoidance system with respect to different hydrometeorological conditions; the results were then compared with those of the ship collision avoidance steering system in calm water. This simplified maneuvering model, based on the database of maneuvering parameters, was extremely effective in finding the helm angle for ship collision avoidance in heavy traffic areas. Under adverse hydrometeorological conditions, maneuvering a ship for collision avoidance is more difficult than under calm water conditions because the safety distance is closer when a larger rudder angle is required.

I. INTRODUCTION

The human, environmental, and economical consequences of collisions at sea are key elements of maritime safety in traffic areas. Enhanced support systems for assisting navigators in collision avoidance at sea are essential for maritime safety. Previously, when captain or ship operators needed to avoid ship collisions or entered the harbor, a trial-and-error method was used in conjunction with their navigation experience to handle the ship. Consequently, the occurrence of ship collisions increased as a result of human factors. To improve the safety of ships in traffic areas, an enhanced support tool has been developed in recent decades and used on board to support ship maneuvering planning and ship collision avoidance at sea. For example, the trial maneuver mode in automatic radar plotting aids or the curved headline overlay in the Electronic Chart Display and Information System are extremely simple and based on current ship motion information (Benedict et al., 2008). The most difficult decisions that captain or ship operators must make is predicting the helm angle of a ship during collision avoidance at sea. Benedict et al. (2008) proposed a prediction tool for simulating a ship's motion in fast time using complex dynamic models that display the effects of rudder or engine maneuvers on the ship track. However, this prediction tool requires considerable computational power to support fast-time simulation on board. To overcome this obstacle and quickly predict ship motions at sea, Fang and Yu (2009) developed a simplified equation for the motion model. This linear model can effectively predict the helm angle when using small rudder angles; however, it cannot provide the nonlinear phenomenon in the initial turning rate histories when the rudder angle is greater than ten degrees.

Numerical simulation is used to predict or confirm the maneuvering performance of a ship during the initial design stage; it offers considerable advantages over competing techniques, such as the ability to perform free-running model tests or sea trials. The hydrodynamic derivatives and coefficients in the simulation can either be obtained by model tests or by theoretical calculations based on potential theory or techniques in compu-

Paper submitted 02/19/19; revised 03/26/19; accepted 05/10/19. Author for correspondence: Kun-Yuan Tsai (e-mail: P18031018@ncku.edu.tw).
[1] Department of Systems and Naval Mechatronic Engineering, National Cheng Kung University , Tainan, Taiwan, R.O.C.
[2] Department of Systems Engineering and Naval Architecture, National Taiwan Ocean University, Keelung, Taiwan, R.O.C.

tational fluid dynamics. Another practical tool is the database method, which is expressed by a simple formula for hydrodynamic coefficients. Numerous related studies have been conducted in this field over the last few decades. For example, Norrbin (1971) introduced the equation of motions, Inoue et al. (1981), Clarke et al. (1983), and Kijima (1990) proposed hydrodynamic coefficients, Oltmann (2003) focused on hydrodynamic damping derivatives, and Sugisawa and Kobayashi (2011) developed steering control. Tam et al. (2009) reviewed numerous collision avoidance and path planning methods for ships in close-range encounters. Most research has focused on ship domain techniques and path planning methods based on danger zones that use velocity vectors and closest passing distances.

The second-order model proposed by Nomoto (1957) was used by Fang and Tsai (2014) to represent the turning characteristics of a large container ship with different traffic factors. Real-time simulations of the large container ship entering Kaohsiung's second harbor have been conducted with and without Nomoto's second-order model by four navigation mates. Fang et al. (2018) enhanced the previous ship collision avoidance steering system (Fang and Tsai, 2014) to develop a simulation of nonuniformly moving ships in calm water and a procedure for collision avoidance decision-making. However, environmental effects such as wind, waves, and current are key considerations for ship collision avoidance. This research therefore developed a simulation model of nonuniformly moving ships in various hydrometeorological conditions and established a procedure for collision avoidance decision-making. This simplified maneuvering model, based on the database of maneuvering parameters, is extremely effective in finding the helm angle required for ship collision avoidance in heavy traffic areas.

II. MATHEMATICAL MODEL

To investigate the six degrees of freedom of ship responses when maneuvering, 6-D maneuvering mathematical techniques based on the Maneuvering Modelling Group model developed by Fang and Luo (2006) were used in this study. The USDDC Maneuvering System (UMS) is a real-time simulator that was developed by Fang et al. (2012) for research purposes. The UMS is a 6-D mathematical model that provides seakeeping and maneuvering characteristics and estimates the related hydrodynamic coefficients by using empirical formulas. We developed a database on the basis of published papers and sea trial measurements. The mathematical model is described by three coordinate systems, as shown in Fig. 1. The first is the earth-fixed coordinate system, $O - X_0Y_0Z_0$, which is fixed in the calm water to describe the pattern of the incident wave and potential flow. The ship body coordinate system $G - xyz$ is then fixed at the center of gravity of the ship and moves with the motion of the ship. The third, $G - x'y'z'$, is also fixed at the center of gravity of the ship. However, the plane $Gx'y'$ always remains parallel with the plane OX_0Y_0. The Z_0, **z**, and z' axes are positive for downward movement. X_G, Y_G, and Z_G are the coordinates for

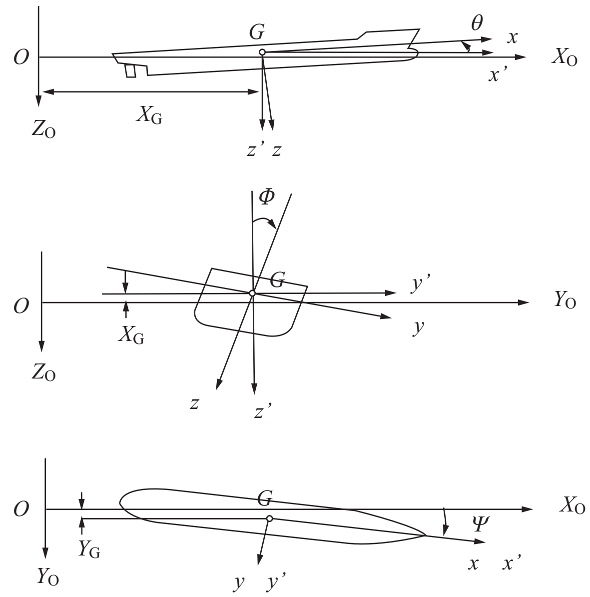

Fig. 1. Global coordinate system (UMS).

the gravity of the ship in the $O - X_0Y_0Z_0$ coordinating system and ϕ, θ, and ψ are Euler's angles.

The horizontal body coordinate system is used to describe the equations of motion. Equations of motion with six degrees of freedom can be written as follows (Fang and Luo, 2006):

$$\begin{aligned} m(\dot{u} - v\dot{\psi}) = {} & (m_y - X_{v\dot{\psi}})v\dot{\psi} - m_x\dot{u} - m_Z w\dot{\theta} + X_{FK} \\ & + X_{RF} + X_{WF} + T(1 - t_p) - R + \mathrm{X_D} + F_{cx} \end{aligned} \tag{1}$$

$$\begin{aligned} m(\dot{v} + u\dot{\psi}) = {} & -m_x u\dot{\psi} - m_y\dot{v} - Y_v v + Y_{\dot{\psi}}\dot{\psi} + Y_{v|v|}v|v| + Y_{v|\dot{\psi}|}v|\dot{\psi}| \\ & + Y_{\dot{\psi}|\dot{\psi}|}\dot{\psi}|\dot{\psi}| + Y_{FK} + Y_{DF} + Y_{RF} + Y_{\mathrm{WF}} + \mathrm{Y_D} + F_{cy} \end{aligned} \tag{2}$$

$$\begin{aligned} m\dot{w} = {} & -m_z\dot{w} - Z_w w + Z_{\ddot{\theta}}\ddot{\theta} - Z_{\dot{\theta}}\dot{\theta} \\ & - Z_\theta\theta + Z_{FK} + Z_{DF} + mg \end{aligned} \tag{3}$$

$$\begin{aligned} I_{xx}\ddot{\phi} - I_{xx}\dot{\theta}\dot{\psi} = {} & J_{xx}\dot{\theta}\dot{\psi} - J_{xx}\ddot{\phi} - K_{\dot{\phi}}\dot{\phi} + (Y_v v - Y_{\dot{\psi}}\dot{\psi})z_H \\ & + K_{FK} + K_{DF} + K_{RF} + K_{\mathrm{WF}} \end{aligned} \tag{4}$$

$$\begin{aligned} I_{yy}\ddot{\theta} + I_{xx}\dot{\psi}\dot{\phi} = {} & -J_{xx}\dot{\phi}\dot{\psi} - J_{yy}\ddot{\theta} - M_{\dot{\theta}}\dot{\theta} + M_\theta\theta \\ & - M_{\dot{w}}\dot{w} - M_w w + M_{FK} + M_{DF} \end{aligned} \tag{5}$$

$$\begin{aligned} I_{zz}\ddot{\psi} - I_{xx}\dot{\theta}\dot{\phi} = {} & J_{xx}\dot{\theta}\dot{\phi} - J_{zz}\ddot{\psi} - N_{\dot{v}}\dot{v} - N_v v - N_{\dot{\psi}}\dot{\psi} + N_{\dot{\psi}|\dot{\psi}|}\dot{\psi}|\dot{\psi}| \\ & + N_{vv\dot{\psi}}v^2\dot{\psi} + N_{v\dot{\psi}\dot{\psi}}v\dot{\psi}^2 + N_\phi\phi + N_{v|\phi|}v|\phi| + N_{\dot{\psi}|\phi|}\dot{\psi}|\phi| \\ & + (-Y_v v + Y_{\dot{\psi}}\dot{\psi} + Y_{v|v|}v|v| + Y_{v|\dot{\psi}|}v|\dot{\psi}| + Y_{\dot{\psi}|\dot{\psi}|}\dot{\psi}|\dot{\psi}|)x_H \\ & + N_{FK} + N_{DF} + N_{RF} + N_{\mathrm{WF}} + \mathrm{N_D} + N_C \end{aligned} \tag{6}$$

$$2\pi I_{pp}\dot{n} = Q_E - Q_P \tag{7}$$

where m and I are the ship mass and mass moment of inertia, respectively. X, Y, and Z are external forces with respect to surge, sway, and heave, and K, M, and N are external moments with respect to roll, pitch, and yaw, respectively. u, v, and w are surge, sway, and heave velocities, respectively, and ϕ, θ, and ψ are roll, pitch, and yaw displacements, respectively. In Eqs. (1)-(7), the related sectional added mass and damping coefficients can be calculated using the Frank close-fit method (Fang et al., 1993; Luo, 2001). Additionally, $\left(m_y - X_{v\dot{\psi}}\right)$ can be expressed as $C_m m_y$, and the value of C_m is between 0.5 and 0.75 (Yoshimura and Nomoto, 1978). The terms m_x, m_y, and m_z represent the added masses with respect to x, y, and z axes, respectively. I_{xx}, I_{yy}, and $I_{zz,}$ represent the added moments of inertia with respect to the x, y, and z axes, respectively. J_{xx}, J_{yy}, and J_{zz} are the ship's added mass moments of inertia about each axis of rotation. The maneuvering derivatives of sway and yaw motions can be estimated using empirical formulas (Inoue et al., 1981). The terms I_{PP}, Q_E, and Q_P represent the moment of inertia of the propeller-shafting system, propeller torque, and main engine torque, respectively. The subscripts *FK*, *DF*, *RF*, and *WF* represent the Froude-Krylov forces, diffraction forces, rudder forces, and wind force, respectively. R is the resistance of the ship. X_D, Y_D, and N_D are longitudinal drifting force, lateral drifting force, and drifting moment, respecttively. F_{cx}, F_{cy}, and N_c are the current forces and moment with respect to the direction of the x-axis, y-axis, and z-axis, respectively.

In this study, we incorporate wind, waves, and current as factors into the 6-D equation of motion. Estimations of the wind forces and moments on the ship are based on the following formulas developed by Isherwood (1973).

$$X_{WF} = X_W(\gamma_R)\frac{1}{2}\rho_a A_f V_R^{\,2} \tag{8}$$

$$Y_{WF} = Y_W(\gamma_R)\frac{1}{2}\rho_a A_S V_R^{\,2} \tag{9}$$

$$K_{WF} = K_W(\gamma_R)\frac{1}{2}\rho_a\left(\frac{A_S^{\,2}}{L}\right)V_R^{\,2} \tag{10}$$

$$N_{WF} = N_W(\gamma_R)\frac{1}{2}\rho_a A_S L V_R^{\,2} \tag{11}$$

where X_{WF}, Y_{WF}, $K_{WF,}$ and N_{WF} are the wind forces and moments with respect to surge, sway, roll, and yaw, respectively. X_W, Y_W, $K_{W,}$ and N_W are nondimensional coefficients of the wind forces and moments with respect to the relative wind angle γ_R (Isherwood, 1973). ρ_a is the air density. Depending on ship length, A_S and A_f are the longitudinal and sideward projected areas of the ship hull above the water surface, respectively. V_R is the ship speed relative to wind. K_W is generally small and can be neglected (Isherwood, 1973).

The current forces and moments on the ship are related to the relative speed and direction of the ship and current. These can be expressed as follows:

$$F_{cx} = \frac{1}{2}\rho\left[(V_c\cos\alpha - \dot{x}_G)^2 + (V_c\sin\alpha - \dot{y}_G)^2\right]BdC_{cx} \tag{12}$$

$$F_{cy} = \frac{1}{2}\rho\left[(V_c\cos\alpha - \dot{x}_G)^2 + (V_c\sin\alpha - \dot{y}_G)^2\right]L_{pp}dC_{cy} \tag{13}$$

$$N = \frac{1}{2}\rho\left[(V_c\cos\alpha - \dot{x}_G)^2 + (V_c\sin\alpha - \dot{y}_G)^2\right]L_{pp}^{\,2}dC_{cn} \tag{14}$$

where V_c is the current speed and α is the angle between the current and ship heading. $\dot{x}_G$ and $\dot{y}_G$ are ship speeds with respect to the center of gravity. L_{pp} is the ship length between the perpendiculars. B, d, and ρ are ship breadth, draft, and sea water density, respectively. C_{cx}, C_{cy}, and C_{cn} are the nondimensional coefficients of the forces and moment with respect to the relative angle α obtained from the empirical formulas (Nienhuis, 1986).

To simplify the calculations, the wave direction is assumed to be the same as the wind direction and is related to the Beaufort wind force scale proposed by the Met Office. The mean longitudinal and lateral drifting forces acting on the ship with respect to the wave direction ψ in short-crest waves can be written as (15)-(18):

$$X_D = \left|\bar{F}_D\right|\cos\psi \tag{15}$$

$$Y_D = \left|\bar{F}_D\right|\sin\psi \tag{16}$$

$$F_D = 2\int_{-\frac{\pi}{2}}^{\frac{\pi}{2}}\int_0^{\infty}\left[\frac{F(\omega)}{\mathrm{A}}\right]^2 S_{aa}(\omega)\bullet d\omega d\psi \tag{17}$$

$$N_D = \int_L Y_D(x)\bullet x dx \tag{18}$$

where $\bar{F}_D$ is the mean nonlinear hydrodynamic drifting force on the ship in random waves, $S_{aa}(\omega)$ is the ITTC-1978 wave spectrum (1978), and A is the wave amplitude. The yaw drifting moment N_D can be integrated from the sectional Y_D with respect to the longitudinal center of gravity along the entire length of the ship. The relevant introduction is presented in Lee et al. (2009).

To build the simplified model, we incorporated the second-

Table 1. Principal particulars of the C-3 container ship.

Length Overall (LOA) (m)	333.2
Length Between Perpendiculars (Lpp) (m)	318.2
Breadth Molded (m)	42.8
Block Coefficient (Cb)	0.56
Draft at Aft Perpendicular (m)	10.08
Draft at Forward Perpendicular (m)	3.75
Rudder rate (°/sec)	3.0

order equation of motion proposed by Nomoto (1964) into the numerical model to investigate the turning characteristics of a C-3 container ship. The second-order model is given as follows:

$$T_1T_2\ddot{r}+(T_1+T_2)\dot{r}+r=K\delta+KT_3\dot{\delta} \tag{19}$$

where K, T_1, T_2, and T_3 are the maneuvering indices, r is the turning rate, and δ is the rudder angle. The turning rate r can be solved as follows:

$$r(t)=K\delta\{1-\frac{T_1-T_3}{T_1-T_2}\exp(-\frac{t}{T_1})-\frac{T_3-T_2}{T_1-T_2}\exp(-\frac{t}{T_2})\} \tag{20}$$

III. COMPUTATIONAL RESULTS AND DISCUSSIONS

To validate the maneuvering mathematical model, we selected the sea trial measurements of the C-3 container ship. The general arrangement of the C-3 container ship is shown in Fig. 2, and the principal particulars are provided in Table 1. During the sea trial, the C-3 container ship was in the ballast condition and the wind was in the range of 2 to 4 on the Beaufort scale. The sea trial of ship C-3 was conducted in the Taiwan Strait. The International Maritime Organization (IMO) has established standards for ships' maneuvering characteristics (IMO, 2002) to ensure minimum safety standards. Turning ability is a measure of the ability to turn the ship using 35° rudder angles. The criteria specify that advances at a 90° change of heading should not exceed 4.5 ship lengths and that tactical diameter, which is defined as the transfer at a 180° change of heading, should not exceed 5.0 ship lengths.

Fig. 3 shows the trajectory for a 35° rudder starboard turn of the C-3 container ship traveling at 26.7 kts in deep water conditions. The blue line is calculated by the formula proposed by Inoue et al. (1981), the pink line represents the numerical results of this study, and the red triangle is obtained from the sea trial results. Larger discrepancies were observed between the results reported by Inoue et al. (1981) and those of the sea trial regarding the advance and tactical diameter of the ship. By contrast, the difference between the present method and the sea trial was small regarding measurements of the advance and tactical diameter of the ship. Notably, the measurement for tactical diameter was 1,451 m in the sea trial, whereas it was 883 m according to Inoue et al. (1981), yielding a 39.1% error; the respective measurements for the advance were 1,125 m and 873.8 m, yielding a 22.3%. For the present method, the measured tactical diameter and advance were 1,512.1 m and 1098.5 m, yielding a 4% error and 2.4% error, respectively, compared with the sea trial results. These results demonstrate that the model for the present method provides a significant improvement for the trajectory of the C-3 container ship. All results satisfy the IMO standards and are listed in Table 2 and Table 3.

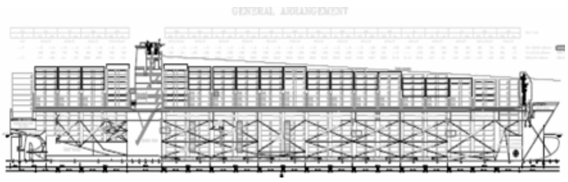

Fig. 2. General arrangement of the C-3 container ship.

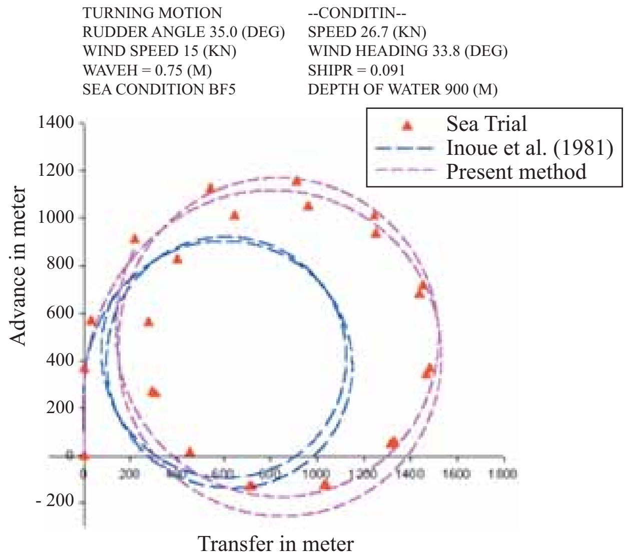

Fig. 3. Trajectory of 35° starboard turn for C-3 container ship.

Table 2 presents a comparison of the validation results for the turning circle test between Inoue et al. (1981) and the sea trial. Considerable error is apparent in the advance, transfer, and tactical diameter measurements of the ship using the method proposed by Inoue et al. (1981).

Table 3 compares the validation results of the turning circle test for the present method with those of the sea trial. Sufficient correlations are apparent in the initial turning stage, along with an adequate improvement of results in the steady turning situation compared with the calm water condition (Fang et al., 2018).

After validating the turning characteristics of the C-3 container ship, a series of related numerical results were obtained using the UMS system.

In 2018, Fang et al. (2018) developed the $K_{(c\text{-}w)}$, $T_{1(c\text{-}w)}$, $T_{2(c\text{-}w)}$, and $T_{3(c\text{-}w)}$ regression models for calm water. These are as follows:

$$K_{(cw)}=0.0026786+0.0034353U-0.0007928\ln\delta\bullet U \tag{21}$$

Table 2. Comparison of starboard turning circle test results for the C-3 container ship between the method proposed by Inoue et al. (1981) and the sea trial.

		Sea Trial results		Inoue et al. results		Error
Starboard	Advance	1125 m	3.54 Lpp	873.8 m	2.75 Lpp	22.3%
	Transfer	543 m	1.71 Lpp	413.3 m	1.3 Lpp	23.9%
	T. Diameter	1451 m	4.56 Lpp	883 m	2.77 Lpp	39.1%

Table 3. Comparison of starboard turning circle test results for the C-3 container ship between the present method and the sea trial.

		Sea Trial results		Present method results		Error
Starboard	Advance	1125 m	3.54 Lpp	1099m	3.45 Lpp	2.4%
	Transfer	543 m	1.71 Lpp	636.8 m	2.0 Lpp	14.7%
	T. Diameter	1451 m	4.56 Lpp	1521 m	4.75Lpp	4.0%

$$T_{1(cw)} = 60.0147\text{-}1.6614\delta - 2.5329U + 0.0325\delta U + 0.0237\delta^2 + 0.035U^2 \tag{22}$$

$$T_{2(cw)} = -170.860236 + 5652.188596\ /U + 58.890545\ln(\delta) - 1401.216267\ln(\delta)/U \tag{23}$$

$$T_{3(cw)} = -88.563572 + 3262.016155\ /U + 4.783375\delta - 76.527108\delta/U \tag{24}$$

where *cw* refers to calm water, U is the ship speed, and δ is the rudder angle.

Various hydrometeorological conditions with respect to wind, waves, and current were considered in the simulation model. The regression models of $K_{(h\text{-}m)}$, $T_{1(h\text{-}m)}$, $T_{2(h\text{-}m)}$, and $T_{3(h\text{-}m)}$ in various hydrometeorological conditions were then constructed. The K value was obtained from the numerical simulations using the regression technique with respect to three forward speeds (10, 14.55, and 20.12 kts), rudder angles (5° to 35°), wind directions (0° to 360°), wind speeds (0 to 22 kts), current directions (0° to 360°), and current speeds (0 to 2 kts). The maneuvering indices $T_{1(h\text{-}m)}$, $T_{2(h\text{-}m)}$, and $T_{3(h\text{-}m)}$ were solved using MATLAB software by employing the Newton-Raphson method to solve the nonlinear equation and using the data obtained from numerical simulations. We then used the regression technique with three forward ship speeds (10, 14.55, and 20.12 kts), four rudder angles ranging from 5° to 35°, four wind directions ranging from 0° to 360°, three wind speeds (10, 15.55, and 22 kts), current directions from 0° to 360°, and two current speeds (1 and 2 kts) to obtain the following equations:

$$K_{(h-m)} = -0.021205 + 0.0059232\ln\delta + 0.0042093U + 0.0009408WS - 0.0009678\ln\delta \bullet U \text{-}0.0002562\ln\delta \bullet WS - 0.000007529\ln\delta \bullet WD - 0.000014036\ U \bullet WS + 0.0000023421 WS \bullet WD \tag{25}$$

$$T_{1(h-m)} = 57.4302\text{-}16.9503\ln\delta - 1.396U + 17.7103\ln WS + 0.1758WD + 0.0082CD + 5.881CS - 0.00203U \bullet WD - 0.2627U \bullet CS - 0.0323\ln WS \bullet WD \tag{26}$$

$$T_{2(h-m)} = -43.42553 + 256.91792/\delta + 2.71223U + 3.10888WS + 0.04615WD - 0.0127CD + 0.21608CS - 12.83881U/\delta + 3.65468WS/\delta + 0.20385WD/\delta - 0.13838U \bullet WS - 0.00155U \bullet WD - 0.00274WS \bullet WD \tag{27}$$

$$T_{3(h-m)} = 70.2395 + 231.4114/\delta - 3.4374U + 1.1212WS + 0.0962WD + 0.0152CD - 5.145CS + 0.4113U \bullet CS - 0.0028WS \bullet WD \tag{28}$$

where "h-m" refers to hydrometeorology; the calculation also involves ship speed (U), rudder angle (δ), wind speed (WS), wind direciton (WD), current speed (CS), and current direction (CD).

To avoid obtaining incorrect values for K, T_1, T_2, and T_3, U was limited to 10-20.12 kts, δ was restricted to 5°-35°, WS was restricted to 10-22 kts, and CS was restricted to 1-2 kts for the regression model of the C-3 container ship.

Figs. 4-7 present the results of comparing these regression models under different hydrometeorological conditions. As indicated in Fig. 4, considerable discrepancies exist between $K_{(h\text{-}m)}$ and $K_{(c\text{-}w)}$ values. The reason for this is that the WS also plays a significant role in Eq. (25), except for the ship speed and rudder angle.

$T_{1(h\text{-}m)}$ and $T_{1(c\text{-}w)}$ regression models are compared in Fig. 5. According to Eq. (26), in addition to the ship speed and rudder angle, wind speed and current speed also have significant effects on the $T_{1(h\text{-}m)}$ regression model. This shows the critical effect that different hydrometeorological conditions have on ship maneuvering.

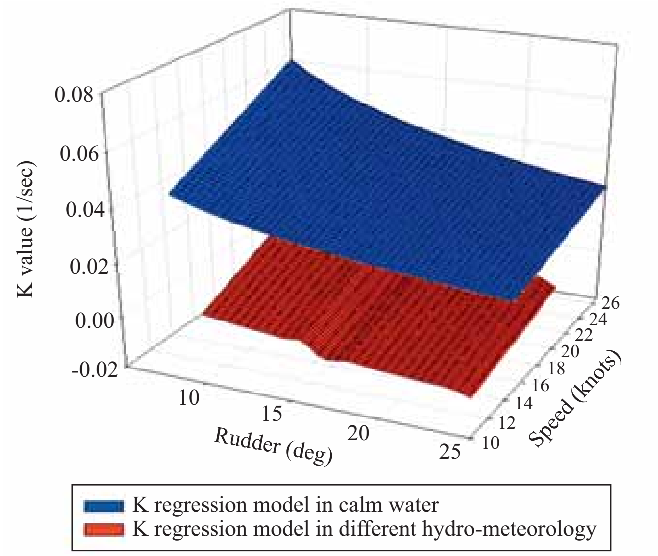

Fig. 4. Comparing the regression model of K(cw) and $K_{(h-m)}$ for the C-3 container ship.

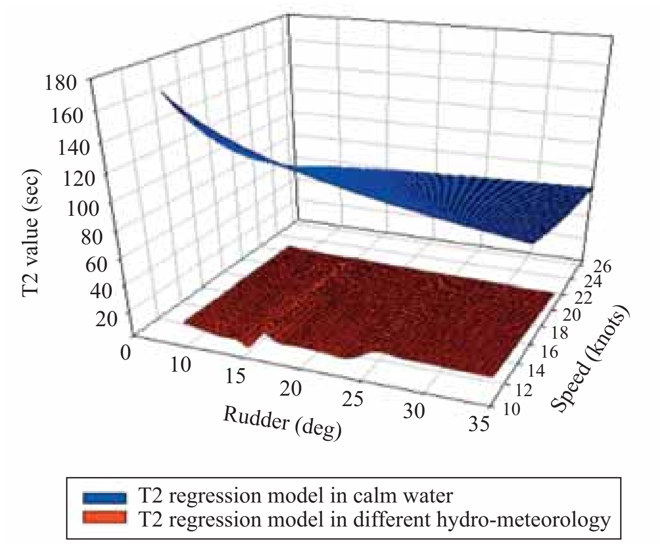

Fig. 6. Comparing the regression model of K(cw) and $T_{2(h-m)}$ for the C-3 container ship.

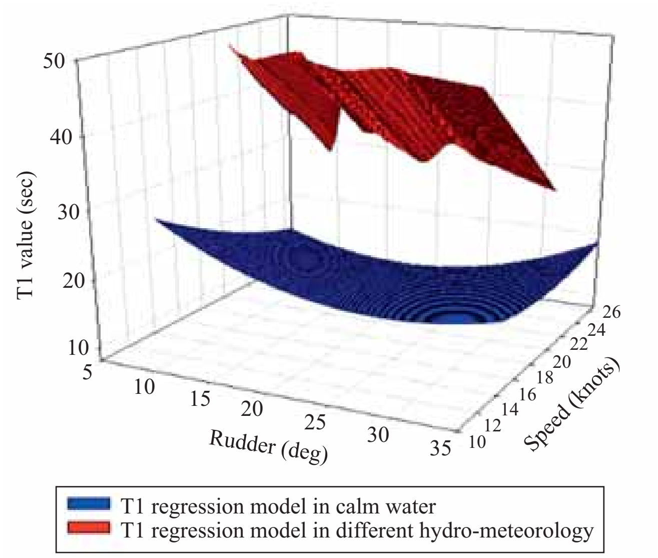

Fig. 5. Comparing the regression model of T_1(cw) and $T_{1(h-m)}$ for the C-3 container ship.

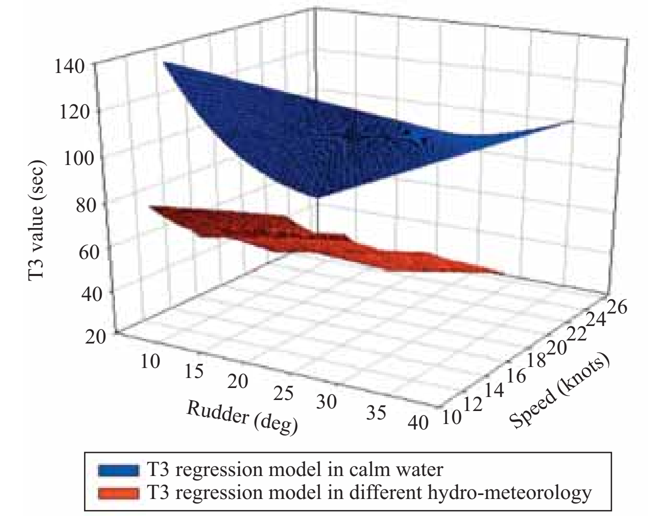

Fig. 7. Comparing the regression model of T_1(cw) and $T_{3(h-m)}$ for the C-3 container ship.

Similar findings can be observed in Figs. 6 and 7.

In this study, we assumed that the current factor is uniform flow for the large container ship. From the results of the numerical simulations in fast time, the current force shows a small influence on ship motion and ship maneuvering compared with wind and wave force.

The ship's collision avoidance steering system in calm water can effectively predict the ship's movement at low speeds with large rudder angles (Fang et al., 2018). When the ship enters a harbor at a low speed, the captain typically employs large rudder angles to maneuver the ship according to personal experience. In this study, we assume that the effective collision avoidance rudder angle was at least 10° for the simulations in the traffic area. The transverse safe domain of the ship was assumed to be 300 m along the side of the moving ships. The proposed ship domain is an ellipsoidal shape at the center of the ship (Fujii and Tanaka, 1971). The safe acting time of the rudder will be at least six times the ship's length (1.0 nautical mile) in advance of the ship in relation to other moving ships in the traffic area. If the distance to the target ship at the action time is less than 1.0 nautical mile, then the initial rudder angle is set to 10°. Fig. 8 presents the flow chart of the optimal helm angle for ship collision avoidance prediction based on the present model. Step 1 of this simulation model involves positioning the target ships, determined by the distance and heading angle, using radar or the

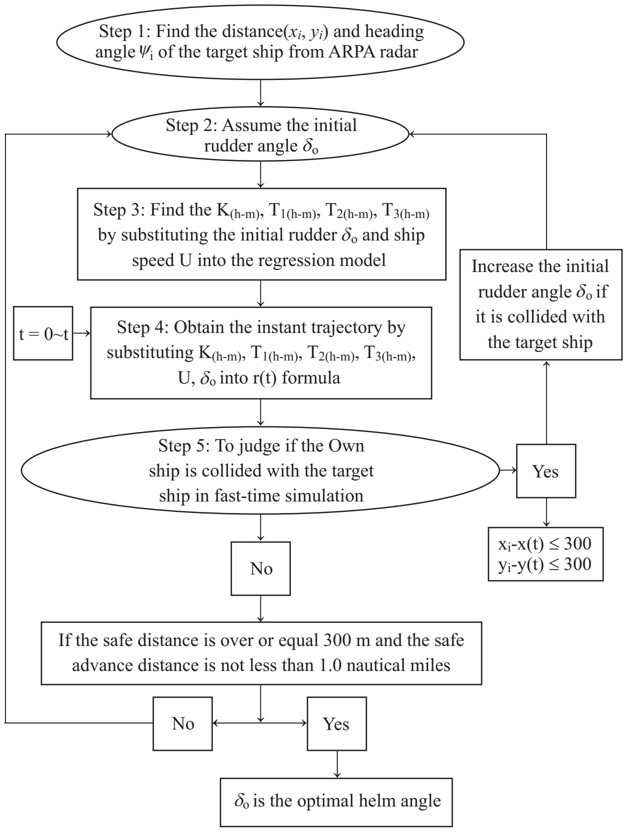

Fig. 8. Optimal helm angle for ship collision avoidance.

Automatic Identification System information on board in each step.

After determining the information for the target ships, step 2 assumes an initial rudder angle δ_0 for the first simulation, and step 3 involves calculating the maneuvering indices $K_{(h\text{-}m)}$, $T_{1(h\text{-}m)}$, $T_{2(h\text{-}m)}$, and $T_{3(h\text{-}m)}$ from Eqs. (25)-(28). These calculations are based on U, the initial rudder angle (δ_0), *WD*, *WS*, *CD*, and *CS*. These are established in advance using the Newton-Raphson method with respect to the three forward ship speeds, four rudder angles, four wind headings, three wind speeds, four current headings, and two current speeds from the UMS simulations. The instantaneous trajectories of the ship are obtained in step 4 by substituting $K_{(h\text{-}m)}$, $T_{1(h\text{-}m)}$, $T_{2(h\text{-}m)}$, $T_{3(h\text{-}m)}$, U, δ, *WD*, *WS*, *CD*, and *CS* into Eq. (20). Based on the predicted trajectories of the ship and numerical recursion techniques, step 5 of the simulation model involves judging whether the ship has collided with the target ships by using a fast-time simulation to examine its helm angle. If the ship has collided with the target ships, the simulation model increases the initial rudder angle, δ_0, by 1-degree intervals. If it is too far away from the target ships, then the model will decrease the initial rudder angle, δ_0, by 1-degree intervals. This is a fast-time simulation process for collision avoidance. Until the helm order reaches the optimal conditions for a safe and energy-efficient navigation route, namely when the safe domain is set at 300 m or the safe advance distance is at 1 nautical mile, the rudder operates on the basis of the helm order. After the ship reaches a position at a safe distance, the

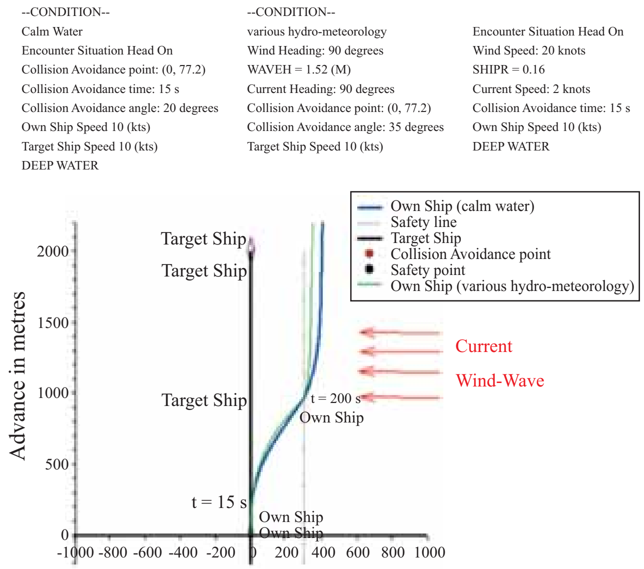

Fig. 9. Ship trajectory for the head-on condition of two nonuniformly moving ships.

rudder angle should follow the helm order to turn back to the initial course according to an autopilot algorithm.

To verify the ship collision avoidance system with respect to the different hydrometeorological conditions, simple and complex collision avoidance cases were designed in fast-time simulations with multiship encounter conditions, and the results were compared with a well-developed ship collision avoidance steering system for calm water. This study simulated three different collision conditions (head-on, overtaking, and crossing situations) with two or three nonuniformly moving ships by using the ship collision avoidance system. In the following simulations, we used slow ahead speed (10 kts) to simulate the cases because the ships are in heavy traffic areas; however, our model can be applied for simulations at higher speeds. The target vessel was only maneuvering in a simple model, the target ships did not take the International Regulations for Preventing Collisions at Sea (COLREGS) into account, and we assumed target ships maintain constant course and speed by applying autopilot to counter hydrometeorological effects. The helm order was calculated using the numerical model and commented on by the captain, and the rudder angle was read from the rudder angle indicator of the ship in this study. All simulation cases for head-on, overtaking, and crossing, and decision-making regarding collision avoidance followed the 1972 COLREGS.

1. Head-On Condition (Simple)

Fig. 9 shows a ship's trajectory for the head-on condition of two nonuniformly moving ships in various hydrometeorological and calm water conditions. The C-3 container ship is traveling at a speed of 10 kts with a heading of 0° (northward). The target ship is 2,000 m in front of the ship and sails at a course of 180° (southward) at 10 kts. In the head-on condition, the C-3 container ship should alter its course to starboard so

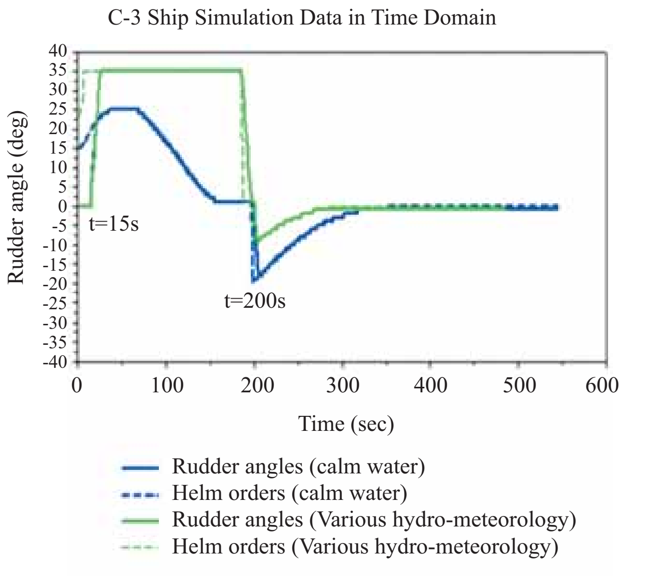

Fig. 10. Time history of the predicted helm order and rudder operation of the head-on condition.

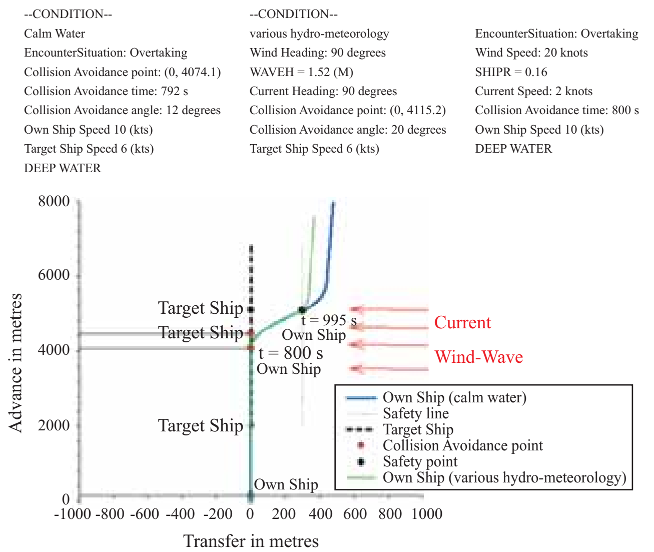

Fig. 11. Ship's trajectory for the overtaking condition of two nonuniformly moving ships.

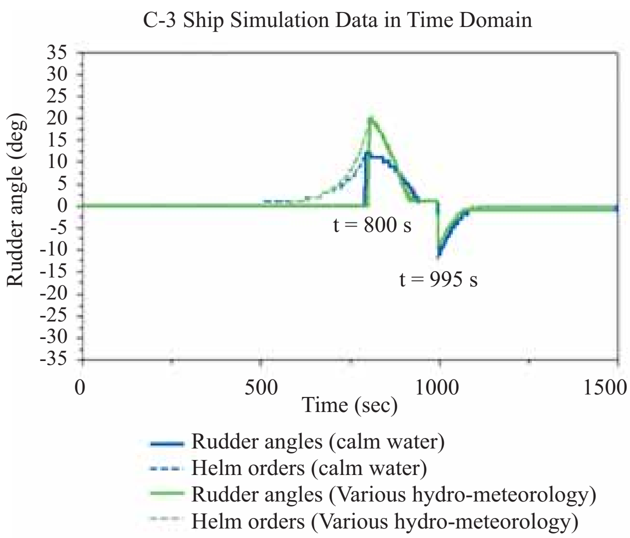

Fig. 12. Time history of the predicted helm order and rudder operation of the overtaking condition.

that each ship passes on the port side of the other (COLREGS 1972, rule 14). Based on the prediction of the present ship collision avoidance model under the conditions of a wind heading of 90°, *WS* of 20 kts, and wave height of 1.52 m, the time for collision avoidance is t = 15 s and the optimal rudder angle is 35°. With this helm order, the ship starts to operate the rudder to sail until it remains 300 m away from the target ship and turns back to its initial northward course. However, the optimal rudder angle is only 20°, as predicted by the ship collision avoidance model in calm water. This shows the effects of various hydrometeorological conditions on ship collision avoidance in heavy traffic areas.

Fig. 10 shows the time history of the predicted helm order and rudder operation for the hydrometeorological and calm water models in a head-on situation. In a hydrometeorological model, although the predictions of the helm order are calculated from the initial simulation, the rudder is kept still until the predicted helm order reaches the optimal angle of 35°, namely at the collision avoidance time t = 15 s. During the simulation, the system model continues to calculate and modify the helm order at each point in time, as shown in Fig. 8. The ship's trajectory is followed by the rudder operation until the ship reaches the safe position, namely a distance of 300 m from the portside of the target ship at around t = 200 s. The autopilot algorithm is then used to return the ship to its initial course. This shows that the prediction of the optimal rudder angle in the hydrometeorological condition is more accurate than the prediction in calm water conditions. Under the effects of wind, waves, and current, the maneuvering of the ship for collision avoidance is more difficult than in calm water, as shown in Fig. 9.

2. Overtaking Condition (Simple)

According to rule 34 of COLREGS (1972), the C-3 container ship may overtake the target ship on either side as long as it indicates its intention by sending clear signals with a whistle. In this study, the starboard side overtaking scenario is selected for discussion. The overtaking condition in Fig. 11 demonstrates that the ship is traveling at 10 kts with a heading of 0°; the target ship is 2,000 m away and maintains its course at a speed of 6 kts in various hydrometeorological and calm water situations. The time for collision avoidance is set at t = 800 s, and the optimal rudder angle is 20°, as predicted by the ship collision avoidance model in various hydrometeorological conditions. The time for collision avoidance is at t = 792 s, and the optimal rudder angle is 12°, as predicted by the ship collision avoidance model in calm water conditions. When the ship reaches the safe location, namely 300 m to the right of the target ship, it returns

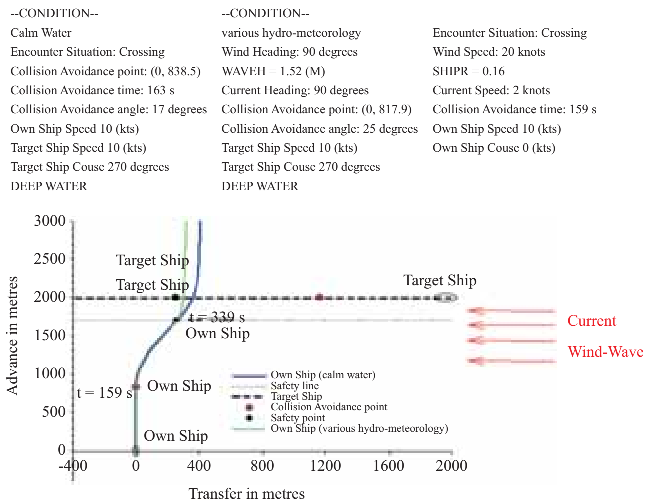

Fig. 13. Ship trajectory for the crossing condition of two nonuniformly moving ships.

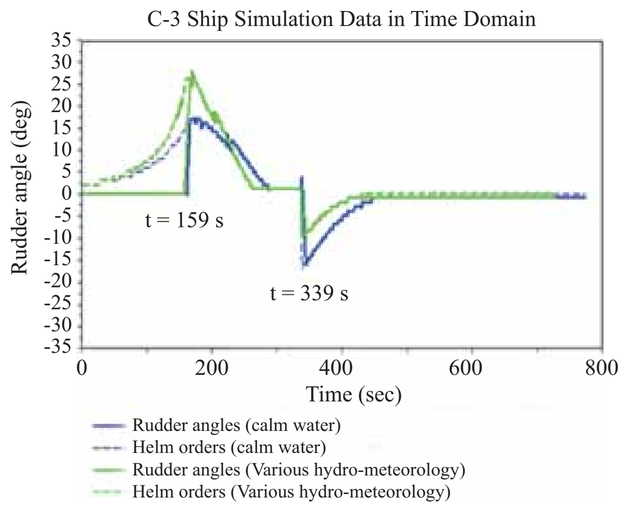

Fig. 14. Time history of the predicted helm order and rudder operation of the crossing condition.

to its original course. When affected by adverse hydrometerological conditions, the maneuvering of the ship for collision avoidance is more difficult than in calm water because the safety distance in hydrometeorological conditions is closer.

Fig. 12 also shows the time history of the predicted helm order and rudder operation for the overtaking condition.

3. Crossing Condition (Simple)

Fig. 13 indicates that the C-3 container ship is traveling at 10 kts with a heading of 0°. The target ship's speed is 10 kts and its heading is 270°, namely approaching from the starboard side of the container ship at the point x_i = 2,000 m and y_i = 2,000 m (the real distance is 2,828 m). According to the Convention on the International Regulations for Preventing Collisions at Sea (COLREGS), the C-3 container ship is the give-way vessel and the target ship is the stand-on vessel. The C-3 container ship should take action to avoid a collision, and the target ship should stay on a steady course. The predicted collision avoidance time and optimal rudder angles are 159 s and 25°, respectively, as calculated by the present ship collision avoidance model in different hydrometeorological conditions. The predicted collision avoidance time and optimal rudder angle in calm water conditions are 163 s and 17°, respectively.

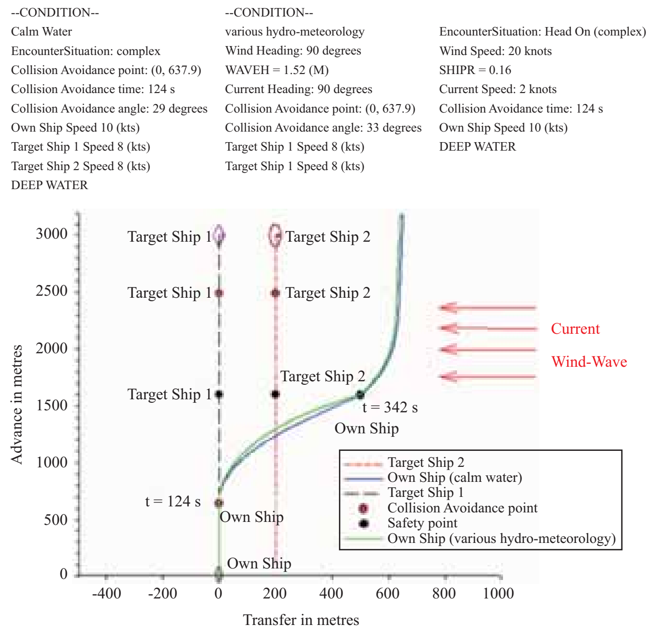

Fig. 15. Ship trajectory for the head-on condition of three nonuniformly moving ships.

Fig. 14 shows the time histories of the predicted helm order and rudder operation, which indicate that the ship maintains its course until the helm order reaches the optimal rudder angle of 25°.

These three simulation results indicate that the helm angles obtained from ship collision avoidance models in various hydrometeorological conditions are larger than that obtained by the model in calm water. This model can also provide a suitable helm order for the C-3 container ship to pass the target ship safely in various hydrometeorological conditions.

Two complex collision conditions, namely head-on and crossing conditions, were then selected for three nonuniformly moving ships to verify the accuracy of the ship collision avoidance system model in various hydrometeorological conditions. The results were compared with those of a well-developed ship collision avoidance steering system for calm water (Fang et al., 2018).

4. Head-On Condition (Complex)

Fig. 15 indicates that the ship is traveling at 10 kts with a heading of 0°. Two target ships are located 3,000 m in front of the ship, and the clearance between the two ships is 200 m. The traveling speed and heading for both target ships are set at 8 kts and 180°, respectively. In this case, we assume the safe distance is at least 300 m from each target ship; therefore, the ship can only sail away to the portside of target ship 2 to avoid colliding with both target ships. The time for collision avoid-

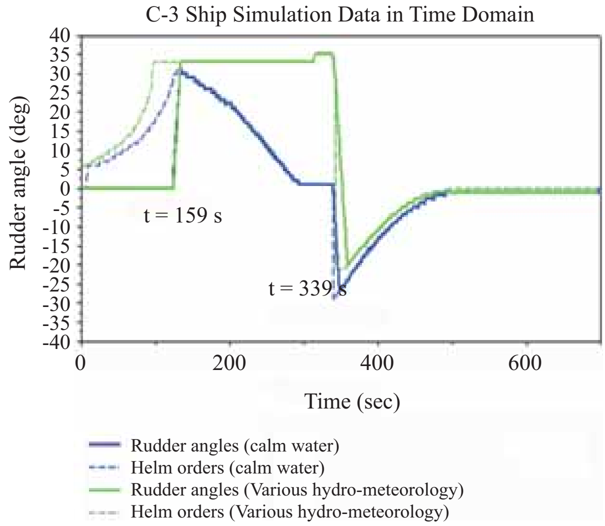

Fig. 16. Time history of the predicted helm order and rudder operation of the head-on condition.

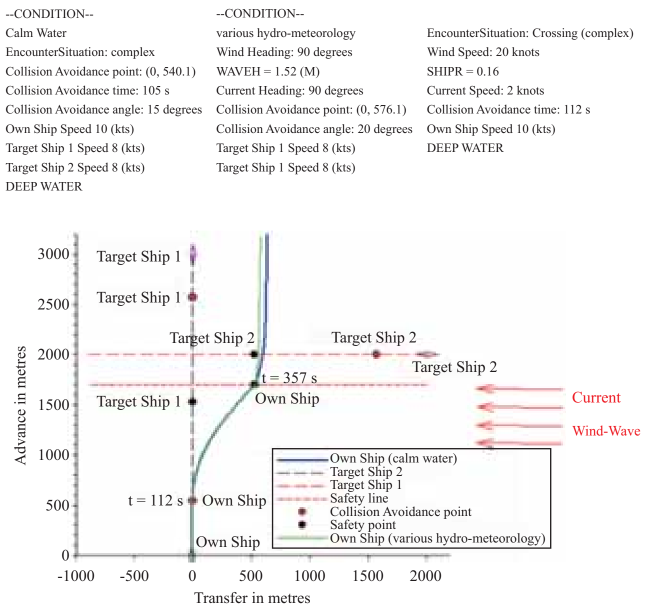

Fig. 17. Ship trajectory for the crossing condition of three nonuniformly moving ships.

ance action is t = 124 s, and the optimal rudder angle is 33°, as predicted by the various hydrometeorological models. The predicted collision avoidance time and optimal rudder angle in the calm water model are 124 s and 29°, respectively.

Fig. 16 presents the time history of the predicted helm order and rudder operation.

5. Crossing Condition (Complex)

The complex crossing condition in Fig. 17 indicates that the ship is traveling at 10 kts with a heading of 0°. Target ship 1 is located 3,000 m in front of the C-3 container ship with a heading of 180° and a speed of 8 kts. Target ship 2 approaches from

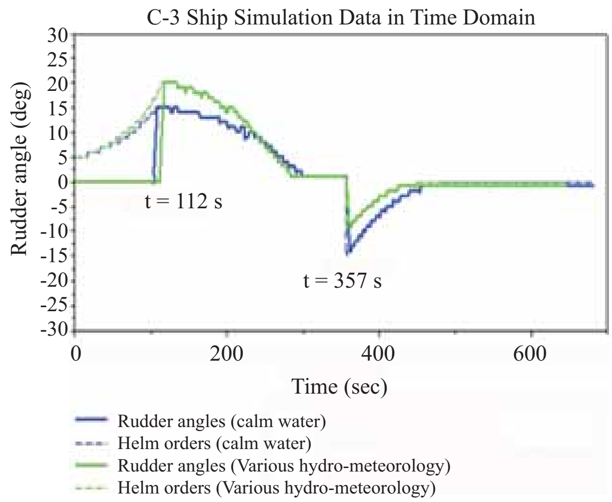

Fig. 18. Time history of the predicted helm order and rudder operation of the crossing condition.

the starboard side of the ship at the point x_i = 2,000 m, y_i.= 2,000 m (the real distance is 2,828 m), a heading of 270, and a speed of 8 kts. The ship collision avoidance system determines which target ship is more dangerous. In this case, if the advance distance of target ship 1 is more than 1 nautical mile from the C-3 container ship, then target ship 2 is considered more dangerous. According to COLREGS, the C-3 container ship is the give-way vessel and target ship 2 is the stand-on vessel. Therefore, the give-way ship should take action to avoid a collision, and the target ship should maintain its course. According to the calculations by the ship collision avoidance model under various hydrometeorological conditions, the time for taking collision avoidance action is t = 112 s, and the optimal rudder angle is 20°. By contrast, the time for collision avoidance action predicted by the calm water model is t = 105 s, and the optimal rudder angle is 15°.

Fig. 18 shows the time history of the predicted helm order and rudder operation.

Based on the two complex simulation results, we can verify that the ship collision avoidance model can be easily applied for various hydrometeorological conditions to obtain the optimal rudder angle with respect to complex conditions for allowing a ship to pass target ships safely.

Based on the verification results of both simple and complex collision avoidance cases, simulations in different hydrometeorological conditions indicate that wind, waves, have significant influences on ship motion and ship maneuvering. The verification results demonstrate that the ship collision avoidance model based on the database of maneuvering indices is effective under various hydrometeorological conditions for obtaining the optimal rudder angle required for ship collision avoidance in a heavy traffic area.

IV. CONCLUSIONS

This study developed a simplified simulation model for use with various hydrometeorological conditions to enhance the safety of ship navigation. We used a real-time simulator for the numerical simulation of a large container ship. To clarify the validity of the proposed maneuverability prediction system, sea trial results for the container ship were compared with the results of the present simulation system in terms of turn trajectory under various hydrometeorological conditions. According to the numerical investigation of turning motion characteristics of a C-3 container ship with various forward speeds, rudder angles, wind directions, wind speeds, current directions, and current speeds, the second-order model proposed by Nomoto (1957) was used to investigate the turning characteristics of the C-3 container ship in this study. Nomoto's second-order model was then incorporated into a numerical model to simplify the turning characteristics of the large container ship for the collision avoidance model. The maneuvering indices can then be obtained from numerical simulations by employing a regression technique. These maneuvering indices form the knowledge base for a simplified simulation model of ships with respect to the effects of various hydrometeorological conditions.

To verify the effectiveness of the ship collision avoidance system under different hydrometeorological conditions, simple and complex collision avoidance cases were designed in fast-time simulations under multiship encounter conditions. The results were compared with those of the ship collision avoidance steering system in calm water. It can be concluded that the simplified simulation model with various hydrometeorological conditions can easily calculate the optimal rudder angle required for ship collision avoidance in heavy traffic areas. Under adverse hydrometeorological conditions, maneuvering a ship for collision avoidance is more difficult than in calm water conditions because the safety distance is closer when a larger rudder angle is required. Wind, waves, and current therefore all have critical effects on ship motion and maneuvering when engaging in ship collision avoidance in heavy traffic areas.

ACKNOWLEDGMENTS

The authors wish to thank the Ministry of Science and Technology, Republic of China (MOST-104-2221-E-006-199-MY3), for its financial support.

REFERENCES

Benedict, K., M. Kirchhoff, M. Baldauf, M. Gluch and S. Fischer (2008). On-board prediction display based on manoeuvring simulation and ship condition. 35th Annual General Meeting of the International Marine Simulator Forum, Sep. 8-12, Rostock-Warnemuende Germany.

Clarke, D., P. Gedling and G. Hine (1983). The application of manoeuvring criteria in hull design using linear theory. Transactions of RINA, 45-68.

Convention on the international Regulations for Preventing Collisions at Sea (1972).

Fang, C. C. and K.T. Yu (2009). Numerical Study on the validation of Turning Characteristics for a Large Container Ship. Proc. of the 9th Asia Conference on Marine Simulator and Simulation Research, June 25-26, Daejeon, Korea.

Fang, C. C. and K. Y. Tsai (2014). An Application of Collision Avoidance System for a Container Ship with Real-Time Simulator. Proc. of the 14th Asia Conference on Marine Simulator and Simulation Research, August 28-29, Tainan, Taiwan.

Fang, M.-C., K. Y. Tsai and C. C. Fang (2018). A Simplified Simulation Model of the Ship Navigation for Safety and Collision Avoidance in Traffic Area. Journal of Navigation, 71, 837-866.

Fang, M.-C., M. L. Lee and C. K. Lee (1993). The simulation of water shipping for a ship advancing in large longitudinal waves. Journal of ship research 37, 26-137.

Fang, M.-C. and J.-H. Luo (2006). On the Track Keeping and Roll Reduction of the Ship in Random Waves Using Different Sliding Mode Controllers. Ocean Engineering 34(3-4), 470-488.

Fang, M.-C., C. C. Fang, C. H. Yen and M. Y. Chen (2012). Numerical Investigation in the Turning Characteristics for a Trimaran in Waves. Proc. of the 12th Asia Conference on Marine Simulator and Simulation Research, August 2-3, Manila, Philippines.

Fujii, Y. and K. Tanaka (1971). Studies in Marine Traffic Engineering: Traffic Capacity, The Journal of Navigation, 24, 543-552.

Isherwood, R. M. (1973). Wind resistance of merchant ships. Transactions of RINA 115, 327-328.

Inoue, S., M. Hirano and K. Kijima (1981). Hydrodynamic derivatives on ship manoeuvring. International Shipbuilding Progress 28(321), 112-125.

International Maritime Organization (2002). Standards for Ship Manoeuvrability. Resolution MSC.137(76).

International Towing Tank Conference (1978). Recommended Procedures and Guidelines.

Kijima, K., Y. Nakiri, Y. Tsusui and M. Matsunaga (1990). Prediction Method of Ship Manoeuvrability in Deep and Shallow Waters. MARSIM & ICSM 90, Tokyo, Japan.

Luo, J.-H. (2001). Directional stability and motions of a ship in severe following waves, Master Thesis (in Chinese), Department of Naval Architecture and Marine Engineering, National Cheng Kung University, Tainan, Taiwan.

Lee, Z.-Y., M.-C. Fang, Y.-Z. Zhuo and Y.-C. Kao (2009). The neural network application on the dynamic position control for a barge using portable hubless thrusters in random waves, TEAM2009, Kaohsiung, 146-152.

Nomoto, K., K. Taguchi, K. Honda, S. Hirano (1957). On the steering quality of ships. International Shipbuilding Progress 4, 354-370.

Nomoto, K. (1964). Ship manoeuvrability. Journal of the society of Naval Architecture Japan, 322-329.

Norrbin, N. H. (1971). Theory and observations on the use of a mathematical model for ship manoeuvring in deep and confined waters. SSPA, Gothenburg, Sweden, Publication 68.

Nienhuis, Ir. U. (1986). Simulation of low frequency motions of dynamically positioned offshore structures. The Royal Institution of Naval Architects 129, 127-145.

Oltmann, P. (2003). Identification of hydrodynamic damping derivatives-a pragmatic approach MARSIM'03.

Sugisawa, M. and H. Kobayshi (2011). Estimation on ship maneuverability based on the correction between hydrodynamic force and moment. 11th Asian Conference on Marine Simulator and Simulation Research, August 25-26, Kure, Japan.

Tam, C., R. Bucknall and A. Greig (2009). Review of collision avoidance and path planning methods for ships in closed range encounters. The Journal of Navigation 62, 455-476.

Yoshimura, Y. and K. Nomoto (1978). Nodeling of manoeuvring behavior of ships with a prepeller idling, boosting and reversing. Journal of the society of Naval Architects of Japan 144, 57-69.